

Dynamical Coupling Atomistic and Continuum Simulations

Guowu Ren, Dier Zhang and Xin-Gao Gong*

Key Laboratory for Computational Physical Sciences (MOE), Fudan University, Shanghai 200433, China.

Received 23 November 2010; Accepted (in revised version) 8 February 2011

Communicated by Weinan E

Available online 2 August 2011

Abstract. We propose a new multiscale method that couples molecular dynamics simulations (MD) at the atomic scale and finite element simulations (FE) at the continuum regime. By constructing the mass matrix and stiffness matrix dependent on coarsening of grids, we find a general form of the equations of motion for the atomic and continuum regions. In order to improve the simulation at finite temperatures, we propose a low-pass phonon filter near the interface between the atomic and continuum regions, which is transparent for low frequency phonons, but dampens the high frequency phonons.

PACS: 47.11.St, 02.70.-c, 46.40.Ff

Key words: Multiscale method, finite element, phonon filter method.

1 Introduction

Multiscale modeling makes simulations at large length and time scales possible. The concurrent multiscale methods [1–7] usually combine different physical length scales together, such as atomic scale described by interatomic potentials or by a tight binding model and the continuum scale usually described by elastic mechanics. Such methods have made their success in the simulation of static [8–10] or quasistatic [11] properties. However, the coupling between two length scales inevitably introduces an artificial interface, and the existence of such an interface can cause the spurious reflection of phonons [12–14]. The reflection can interfere with the dynamics in the atomic region and thus prohibit the application of the concurrent multiscale methods to properly simulate dynamical properties. Recently, some hybrid methods have taken a step towards in the

*Corresponding author. *Email addresses:* gwren@fudan.edu.cn (G. Ren), dearzhang@fudan.edu.cn (D. Zhang), xggong@fudan.edu.cn (X.-G. Gong)

treatment of dynamical processes [15] by introducing suitable boundary conditions (BC) placed at the coupling interface, such as stadium BC [16,17], exact BC [18–20] and absorbing BC [21], or perfectly matched layer (PML) [22,23]. Such boundary conditions adopt either a time-dependent [18] or position dependent damping term [16], with which all waves are dampened near the interface region.

However, although the physics properties at two length scales themselves are different, the low frequency phonons can exist in both length scale, while the high frequency phonons can only exist in the atomic region. Meanwhile the low frequency phonon plays a significant role in understanding the long range interaction related to mechanical deformation. Hence, the boundary condition should be frequency dependent, and it should be transparent for the phonon with the frequency as high as possible. The previously proposed algorithms [16,18,24] dampen all phonons for the computational convenience. Therefore it is essential to construct a realistic algorithm to couple atomic and continuum simulations.

In this paper, an atomic-based finite element method (AFEM) is introduced, which can be merged seamlessly with an atomistic region in order to enable energy transferring through the coupling interface. Meanwhile, we design a new damping method near the interface to absorb the spurious reflections of high frequency, while keeping low frequency phonons transparent.

2 Theoretical method and analysis

We first consider a one-dimensional (1D) model which can be spatially composed of MD region, FE region and linking region (LR), as shown in Fig. 1. We adopt Lagrangian mechanics to describe the MD region, which is shown without the external force as

$$L(\mathbf{u}, \dot{\mathbf{u}}) = \frac{1}{2} \dot{\mathbf{u}}^T \mathbf{M}_A \dot{\mathbf{u}} - V(\mathbf{u}), \quad (2.1)$$

where \mathbf{M}_A is diagonal mass matrix denoted by atomic mass m_μ and \mathbf{u} is discrete atomic displacement. The MD simulation can be numerically implemented in terms of Newton's equation by solving Eq. (2.1).

The FE region is divided into two-node elements with different length from the lattice length a_μ , which is gradually scaled up to $h_l = n_l a_\mu$ ($n_l = 1, 2, \dots$) into the macroscale, as shown in the left part of Fig. 1. The linear basis functions are set up on the FE region which is linked with the MD systems nearby the most dense elements. Under the Cauchy-Born rule [25], the atomic displacement \mathbf{u} is the linear mapping of the nodal displacement \mathbf{d} , expressed as $\mathbf{u} = \mathbf{J}\mathbf{d}$, where \mathbf{J} is Jacobi matrix of the linear interpolation function which provides the atomic displacement within the element. Substituting this relation into Eq. (2.1), by solving the corresponding Lagrangian equation, the equation of motion can be written as

$$[\mathbf{M}][\ddot{\mathbf{d}}] = -[\mathbf{K}][\mathbf{d}], \quad (2.2)$$

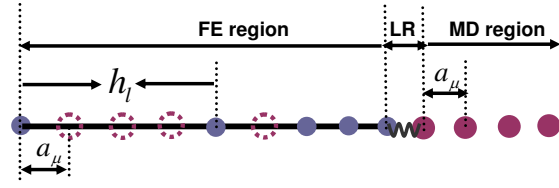


Figure 1: Schematic of a one-dimensional multiscale model which includes the FE region, MD region and linking region (LR).

where $[\mathbf{M}] = \mathbf{J}^T \mathbf{M}_A \mathbf{J}$ is the mass matrix and $[\mathbf{K}] = \partial^2 V(\mathbf{J}\mathbf{d}) / \partial \mathbf{d}^2$ is the stiffness matrix.

Since the conventional FE method [26] is derived from the macroscale continuum constitutive relation, the atomic behavior representing localized bond and discrete mass could not be captured. Although the lumped mass approximation [2] is chosen to match with the discrete distribution of atomic mass, this approximation conflicts with the consistent distribution of mass in the continuous region, which can be greatly improved.

Based on the divided principle of elements, a concrete formalism of mass and stiffness matrix can be obtained. The mass matrix can be formed as a tridiagonal,

$$[\mathbf{M}] = m_\mu \begin{bmatrix} \ddots & & & & & & \\ & \zeta^l & \eta^l & \zeta^l & & & \\ & & \ddots & \ddots & \ddots & & \\ & & & \ddots & \ddots & \ddots & \\ & & & & \ddots & \ddots & \ddots \end{bmatrix}, \quad (2.3)$$

where $\zeta^l = (n_l - 1)(n_l + 1) / 6n_l$, $\eta^l = n_l - 2\zeta^l$ and n_l is number of atoms per element.

The stiffness matrix can be evaluated by the derivative of the interatomic potential, expressed as

$$K_{ij} = \sum_\mu \frac{\partial^2 V(u_\mu)}{\partial d_i \partial d_j}, \quad (2.4)$$

where d_i is the i -th component of \mathbf{d} . For simplicity, the interatomic potential $V(u_\mu)$ is chosen to involve the nearest and second neighbor interactions, and the force constant is separately k_1 and k_2 . Thus the stiffness matrix is given as

$$[\mathbf{K}] = \begin{bmatrix} \ddots & & & & & & \\ & \kappa_\alpha^l & \kappa_\beta^l & \kappa_\gamma^l & \kappa_\beta^l & \kappa_\alpha^l & \\ & & \ddots & \ddots & \ddots & & \\ & & & \ddots & \ddots & \ddots & \\ & & & & \ddots & \ddots & \ddots \end{bmatrix}, \quad (2.5)$$

where

$$\kappa_\alpha^l = \frac{k_2}{n_l^2}, \quad \kappa_\beta^l = \frac{k_1}{n_l} + \frac{4n_l - 4}{n_l^2} k_2, \quad \kappa_\gamma^l = -2(k_\beta^l + k_\alpha^l).$$

This matrix is pentadiagonal, which indicates that the nodal force involves the second neighbor interactions.

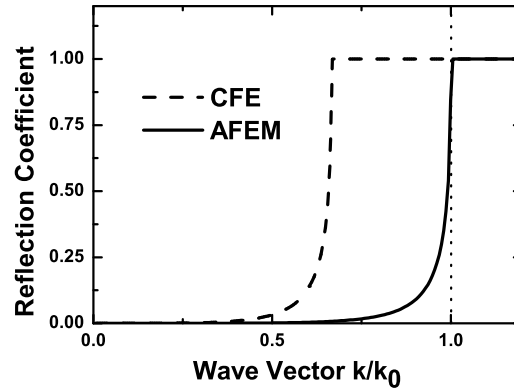


Figure 2: Comparison of the calculated reflection coefficient for AFEM and conventional FE methods with lumped mass approximation. The AFEM can largely improve the transparency.

Hereto we have obtained the equation of AFEM, described by node-dependent mass and stiffness matrix. When the element length equals with lattice length as $n_l=1$, the mass matrix will be reduced to be diagonal and the equation of AFEM is corresponding with the one of atomistic region. And for $n_l = \infty$, the mass and stiffness matrix tends toward tridiagonal and the equation of AFEM becomes the continuous case, where the model approaches linearly elastic medium as the elastic constant is $\mathbf{C} = (k_1 + 4k_2)a_\mu$. Therefore, the present equation of AFEM can seamlessly span from atomistic region to FE region.

Since the present mass matrix is essentially different from the lumped mass matrix used in the conventional method, where the mass of atoms are simply on the two nodes of the element and the matrix is diagonal with equal value of $1/2$. The new mass and stiffness matrix can largely improve the scattering of the varying mesh interface in the FE region. Fig. 2 shows the reflection coefficient of a plane wave with the frequency ω traveling from atomic region to $n_l = 2$ region, compared with conventional FE method with lumped mass matrix approximation. It is clear that, the lower limit of the complete reflection is increased more than 30 per cent. This indicates that more phonon with higher frequency can travel into the FE region and reduce the unphysical energy resistance. However, although the new mass matrix significantly improved the transparency, the spurious phonon reflection still exists at the large wave vector $k_0 \geq \pi/n_l$, one must find out an algorithm to dampen the spurious reflection.

Here we provide a low-pass filter procedure [27] to filter the reflection of high-frequency phonons but keeping the propagation of low frequency ones. In the dynamical process, the vibration of every atom (node) can be seen as a signal where the displacement $u(t)$ changes with time t , analogous to the circuit signal. Therefore we can construct a transfer function defined as $H(s) = u_v(s)/u_{v-1}(s)$ between the neighbor atomic signals, where the variable s is the Laplace transform of time t , which exhibits a frequency response for the different atomic signals. $H(s)$ is an intrinsic quantity strongly dependent on the atomic model and is governed by the dynamical equation.

As an ideal model, the equation of motion for 1D harmonic lattice system only subjected to the nearest-neighbor interaction, in terms of displacement u_ν , can be written as

$$\ddot{u}_\nu(t) = u_{\nu-1}(t) + u_{\nu+1}(t) - 2u_\nu(t), \quad (2.6)$$

where the atomic mass and force constant is set to be 1. Utilizing the Laplace transform, one can obtain the corresponding transfer response $H(s)$, which reads,

$$H(s) = \frac{2 + s^2 - s\sqrt{4 + s^2}}{2}. \quad (2.7)$$

In the frequency space, the module $|H(i\omega)|$ is equal to 1, indicating that all the vibrational modes can travel back and forth without any damping. Note that although the derived consequence of $H(s)$ is under the condition of infinite atomic chain, seen from its definition it describes the local transfer relation between neighbor atoms far away from the boundary. However, to ensure the application of finite damping layers effectively in the practical multiscale simulation, the local transfer function for one damping layer embedding in the infinite linear chain is essentially studied to exhibit the filter property.

To demonstrate the validity of local transfer function, we will illustrate the filter response by Langevin damping method, which has been widely applied for eliminating the wave reflection necessarily occurred in the MD, FE or multiscale simulation boundary, as mentioned in the introduction. Its equation of motion associated with a viscous force, can be described by

$$\ddot{u}_\nu(t) = u_{\nu-1}(t) + u_{\nu+1}(t) - 2u_\nu(t) - \beta\dot{u}_\nu(t), \quad (2.8)$$

where β is the damping coefficient with respect to the highest frequency of phonon dispersion relation. Following the Laplace transform, the Eq. (2.8) can be inverted into the local transfer function for single damping layer

$$H(s) = \frac{2}{s^2 + 2 + s\sqrt{4 + s^2} + 2\beta s}. \quad (2.9)$$

It should be notable that the local transfer relation between atom $\nu+1$ and ν in the ideal harmonic lattice has been employed because of the approximative equivalence of their displacements ratio for ideal and damping model in the time space. Though the atomic vibrated modes induced by nonlinear viscous term will shift, the excited frequencies responsible for boundary reflection are primarily devoted to the long wavelength acoustic modes. In addition, in the practical simulation the damping coefficient β is generally not chosen too large to prevent from the severe wave reflection. Through the simulation technique the amplitude ratio between atom ν and $\nu-1$ concerning the module $|H(i\omega)|$ is numerically calculated and is in good agreement with the analytical result for the small β and vibrated frequencies of Brillouin zone. As well one can evaluate the module $|H(i\omega)|$ involving multiple damping layers, used for estimating roughly the width of damping

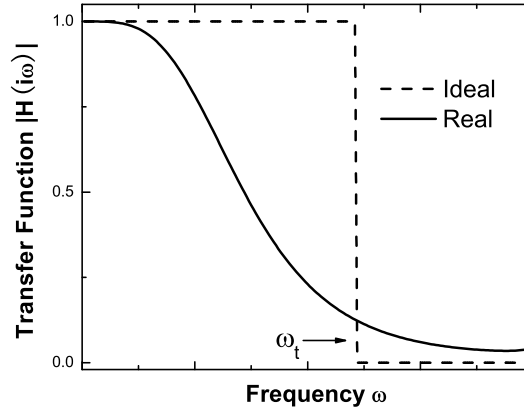


Figure 3: Transfer function for eliminating reflected phonons. ω_t is the minimum frequency of total reflection. The dashed line is the ideal transfer function. The solid line is a realistic transfer function we obtained for a one dimensional system as described by Eq. (2.10).

layers applicable to wave absorption. While the module $|H(i\omega)|$ goes to zero, it indicates that all the waves have been dampened.

However, in our present goal to develop the dynamical multiscale method, a new BC is expected to meet the demand that only the high-frequency waves are eliminated while keeping the low-frequency waves traveling. That is to say, this BC should be frequency-dependent. Nevertheless, Langevin damping method determines the same exponential decay for high-frequency waves or low-frequency, and hence it is not appropriate, as well including the developed damping approaches.

In order to filter out the reflected high frequency phonons, the ideal transfer function should be a step-function as shown in Fig. 3. Unfortunately, although one can write down the theoretical expression of ideal transfer function, it is difficult to be converted into an equation of motion in the time domain. Notwithstanding, it provides a route to approach the solution that one can produce an approximate form of the transfer function which can lead to an equation of motion with properly filter behavior. For instance, as shown in Fig. 3 (solid line), we have successfully designed a realistic low-pass transfer function, which can filter out most of phonons with frequency higher than ω_t in correspondence with on the wave vector k_0 in Fig. 2. The corresponding transfer function for single damping layer is expressed as

$$H(s) = \frac{1 + \beta s}{s^2 + \frac{2 - s^2 + s\sqrt{4 + s^2}}{2}(1 + \beta s)}, \quad (2.10)$$

where β is a parameter which controls the shape of the transfer functions. By carrying out the same deriving procedure as the Eqs. (2.8) and (2.9) and taking an inverse Laplace transform, the resulting equation of motion is shown by

$$\ddot{u}_v = u_{v+1} + u_{v-1} - 2u_v + \beta(\dot{u}_{v+1} + \dot{u}_{v-1} - 2\dot{u}_v). \quad (2.11)$$

Rewriting the Eq. (2.11) for the general case yields

$$\ddot{u}_v = -\frac{\partial V(u_v)}{\partial u_v} + \beta(\dot{u}_{v+1} + \dot{u}_{v-1} - 2\dot{u}_v). \quad (2.12)$$

The second term with damping role in Eq. (2.12) is composed of two-order difference of the velocity between the neighbor atoms, instead of the damping term proportional to the on-site velocity in the Langevin dynamics. By theoretical analysis, we found that this damping form is dependent on the vibrated frequency. Obviously, the present damping mechanism can effectively dampen high frequency phonons which have large two order differences of the velocity, and keep the low frequency phonons which have small two order difference of the velocity. In comparison, as stated earlier, Langevin dynamics dampens nearly all the frequency. We call the present damping scheme as the Phonon Filter (PF) method.

3 Numerical simulation results

In order to show the effectiveness of the AFEM and PF method, we perform a dynamical simulation in the one-dimensional multiscale model, as illustrated in Fig. 1. In the finest part of the FE region, the equation of AFEM is equivalent to the one of MD region so that the dynamical properties can be automatically matched and there is no phonon reflection at the atomistic/continuum interface. The spurious reflection intensively emits from the varied mesh-size interface and PF method can be used to dampen the reflections. The maximum value of element length n_l is up to 2 and the thickness of LR region is chosen to be 6. The velocity-Verlet algorithm is used for time integration for the whole system.

The dynamics of Gaussian wave packets traveling from the MD region to the FE region are also simulated. Fig. 4 shows the obtained results from three different simulation methods: lumped mass FE method, AFEM without any filter scheme and AFEM with PF, as shown in Fig. 4(a), (b) and (c), respectively. The wave-packet with wave vector $k=0.7$ and $k=1.8$, are chosen as the testing wave. For $k=0.7$, there is significant reflection of waves using the lumped mass FE method, however, in the AFEM, the wave-packet is essentially transparent. For the $k=1.8$, the wave-packet is completely not transparent and nothing can be transmitted to FE region. In lumped FE and AFEM, the wave-packet is completely reflected. However, the PF method can completely kill the reflected wave as desired.

By calculating the energy changes between MD and FE region, we can numerically obtain the reflection and transmission coefficient dependent on wave vector. Fig. 5 shows the reflection and transmission coefficient which is plotted as a function of wave vector k for three different simulation methods. The results show that AFEM with PF method can eliminate the reflected phonon of high-frequency and have very little influence on transmission of low-frequency phonon and the lumped mass FE method retains strong reflection. From the reflection coefficient, one can see that most of the spurious reflections

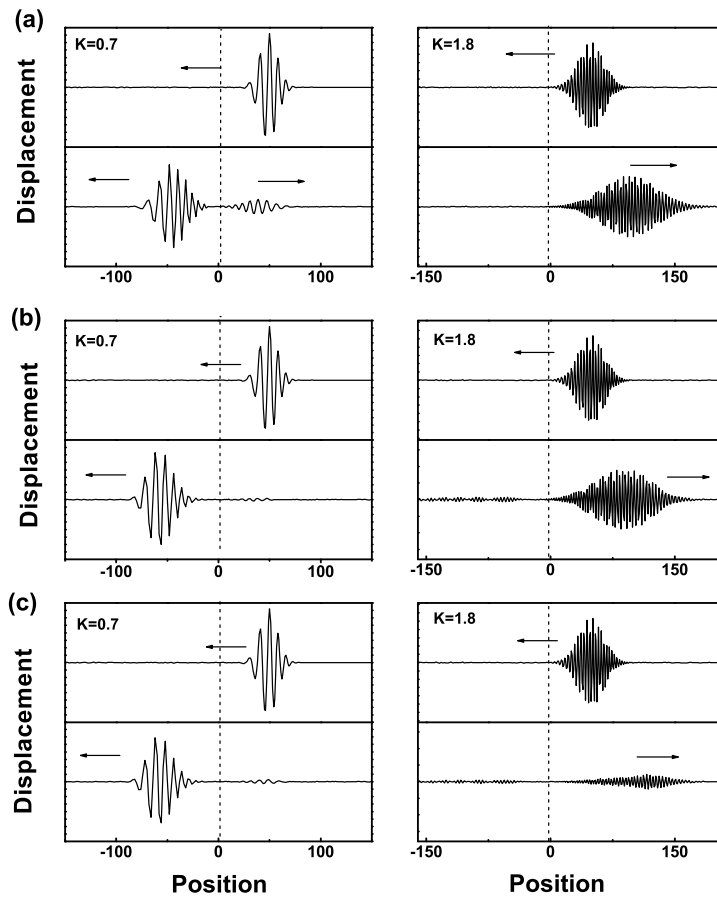


Figure 4: Gaussian wave packet of small wave vector (left column) and large wave vector (right column) travelling from the MD region to FE region. (a) lumped mass FE method; (b) AFEM; (c) AFEM with PF method. The dashed line denotes the atomistic/continuum interface. It is clear that PF has little effect on the small wave vector packet, while it dampens the large wave vector packet.

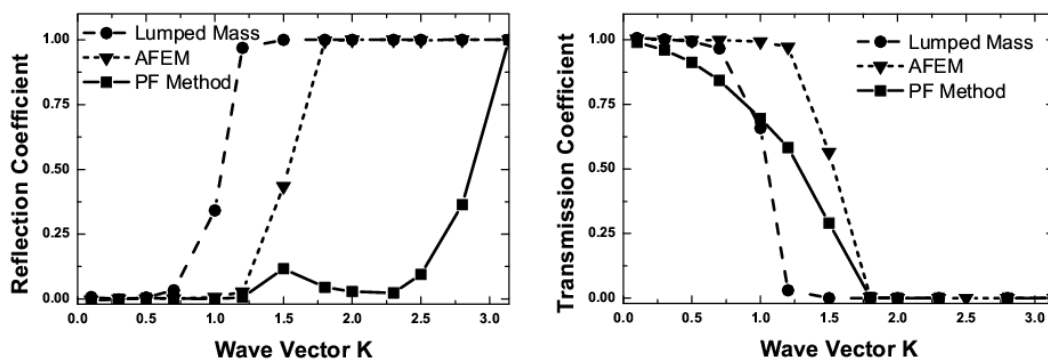


Figure 5: A comparison of reflection and transmission coefficients using numerical simulations. The \blacksquare line, \blacktriangle line and \bullet line are the result of AFEM with PF method, AFEM and lumped mass FE method, respectively.

are eliminated and only a small fraction of wave near $k = 1.5$ remain because the transfer function is still different from a perfect step-function. At the phonon vector $k = 3.0$ close to the Brillouin zone, the velocity of these waves is very slow, so that it is difficult to be dampened out as with other methods.

4 Conclusions

In summary, we have proposed an atomic-based finite element method, which can increase phonon transparency by using a consistent mass matrix and stiffness matrix. The derived equation of motion perfectly match together for the atomic region and continuum region. We have also developed a phonon filter method with a new damping mechanism which is proportional to two-order difference of velocity. The phonon filter can keep high transparency for low frequency phonons and simultaneously dampen the reflected waves of high-frequency. The efficiency is demonstrated by simulating the dynamics of the wave packet, and the reflection and transmission coefficients. The present method is simple but efficient, and we believe that it can open a window for performing high-accuracy multiscale simulations at the dynamical regime.

Acknowledgments

The authors are thankful to Prof. Z. Y. Zhang for the discussions. This work is supported by the National Science Foundation of China, the special funds for major state basic research, and Shanghai municipality and MOE. The computations were performed at Fudan Supercomputer Center.

References

- [1] S. Kohlhoff, P. Gumbsch and H. F. Fischmeister, Crack propagation in b.c.c crystals studied with a combined finite-element and atomistic model, *Phil. Mag. A*, 64 (1991), 851–878.
- [2] J. Q. Broughton, F. F. Abraham, N. Bernstein and E. Kaxiras, Concurrent coupling of length scales: methodology and application, *Phys. Rev. B*, 60 (1999), 2391–1403.
- [3] E. B. Tadmor, M. Ortiz and R. Phillips, Quasicontinuum analysis of defects in solids, *Phil. Mag. A*, 73 (1996), 1529–1563.
- [4] R. E. Rudd and J. Q. Broughton, Coarse-grained molecular dynamics and the atomic limit of finite elements, *Phys. Rev. B*, 58 (1998), R5893–R5896.
- [5] G. J. Wanger and W. K. Liu, Coupling of atomistic and continuum simulations using a bridging scale decomposition, *J. Comput. Phys.*, 190 (2003), 249–274.
- [6] S. P. Xiao and T. Belytschko, A bridging domain method for coupling continua with molecular dynamics, *Comput. Methods Appl. Mech. Eng.*, 193 (2004), 1645–1669.
- [7] D. T. Read and V. K. Tewary, Multiscale model of near-spherical germanium quantum dots in silicon, *Nanotechnology*, 18 (2007), 105402.
- [8] J. Knap and M. Ortiz, Effect of indenter-radius size on Au (001) nanoindentation, *Phys. Rev. Lett.*, 90 (2003), 226102.

- [9] Q. Peng, X. Zhang, L. Hung, E. A. Carter and G. Lu, Quantum simulation of materials at micron scales and beyond, *Phys. Rev. B*, 78 (2008), 054118.
- [10] L. E. Shilkrot, R. E. Miller and W. A. Curtin, Coupled atomistic and discrete dislocation plasticity, *Phys. Rev. Lett.*, 89 (2002), 025501.
- [11] E. Lidorikis, M. E. Bachlechner, R. K. Kalia, A. Nakano and P. Vashishta, Coupling length scales for multiscale atomistics-continuum simulations: atomistically induced stress distributions in Si/Si_3N_4 nanopixels, *Phys. Rev. Lett.*, 87 (2001), 086104.
- [12] B. Q. Luan, S. Hyun, J. F. Molinari, N. Bernstein and Mark O. Robbins, Multiscale modeling of two-dimensional contacts, *Phys. Rev. B*, 74 (2006), 046710.
- [13] Z. P. Bažant, Spurious reflection of elastic waves in nonuniform finite element grids, *Comput. Methods Appl. Mech. Eng.*, 16 (1978), 91–100.
- [14] R. E. Rudd and J. Q. Broughton, Coarse-grained molecular dynamics: nonlinear finite elements and finite temperature, *Phys. Rev. B*, 72 (2005), 144104.
- [15] W. K. Liu, H. S. Park, D. Qian, E. G. Karpov, H. Kadowaki and G. J. Wagner, Bridging scale methods for nanomechanics and materials, *Comput. Methods Appl. Mech. Eng.*, 195 (2006), 1407–1421.
- [16] S. J. Zhou, P. S. Lomdahl, R. Thomson and B. L. Holian, Dynamic crack processes via molecular dynamics, *Phys. Rev. Lett.*, 76 (1996), 2318–2321.
- [17] S. Qu, V. Shastry, W. A. Curtin and R. E. Miller, A finite-temperature dynamic coupled atomistic/discrete dislocation method, *Model. Simul. Mater. Sci. Eng.*, 13 (2005), 1101–1118.
- [18] W. Cai, M. de Koning, V. V. Bulatov and S. Yip, Minimizing boundary reflections in coupled-domain simulations, *Phys. Rev. Lett.*, 85 (2000), 3213–3216.
- [19] W. E and Z. Huang, Matching conditions in atomistic-continuum modeling of materials, *Phys. Rev. Lett.*, 87 (2001), 135501.
- [20] J. Z. Yang and X. Li, Comparative study of boundary conditions for molecular dynamics simulations of solids at low temperature, *Phys. Rev. B*, 73 (2006), 224111.
- [21] S. Namilaie, D. M. Nicholson, P. K. V. V. Nukala, C. Y. Gao, Y. N. Osetsky and D. J. Keffer, Absorbing boundary conditions for molecular dynamics and multiscale modeling, *Phys. Rev. B*, 76 (2007), 144111.
- [22] S. Li, X. Liu, A. Agrawal and A. C. To, Perfectly matched multiscale simulations for discrete lattice systems: extension to multiple dimensions, *Phys. Rev. B*, 74 (2006), 045418.
- [23] R. E. Jones and C. J. Kimmer, Efficient non-reflecting boundary condition constructed via optimization of damped layers, *Phys. Rev. B*, 81 (2010), 094301.
- [24] B. Kraczek, S. T. Miller, R. B. Haber and D. D. Johnson, Adaptive spacetime method using Riemann jump conditions for coupled atomistic-continuum dynamics, *J. Comput. Phys.*, 229 (2010), 2061–2092.
- [25] M. Born and K. Huang, *Dynamical Theories of Crystal Lattices*, Clarendon Press, Oxford, 1954.
- [26] T. J. R. Hughes, *The Finite Element Method: Linear Static and Dynamic Finite Element Analysis*, Prentice-Hall, Englewood Cliffs, NJ, 1987.
- [27] S. K. Mitra, *Digital Signal Processing: A Computer-Based Approach*, McGraw-Hill, 2004.